Vol. 12 No. 3

Nuclear Physics News International

FEATURING:
Lab Portrait Oak Ridge • Critical Point Symmetries • From Nuclear Physics to NMR Tomography

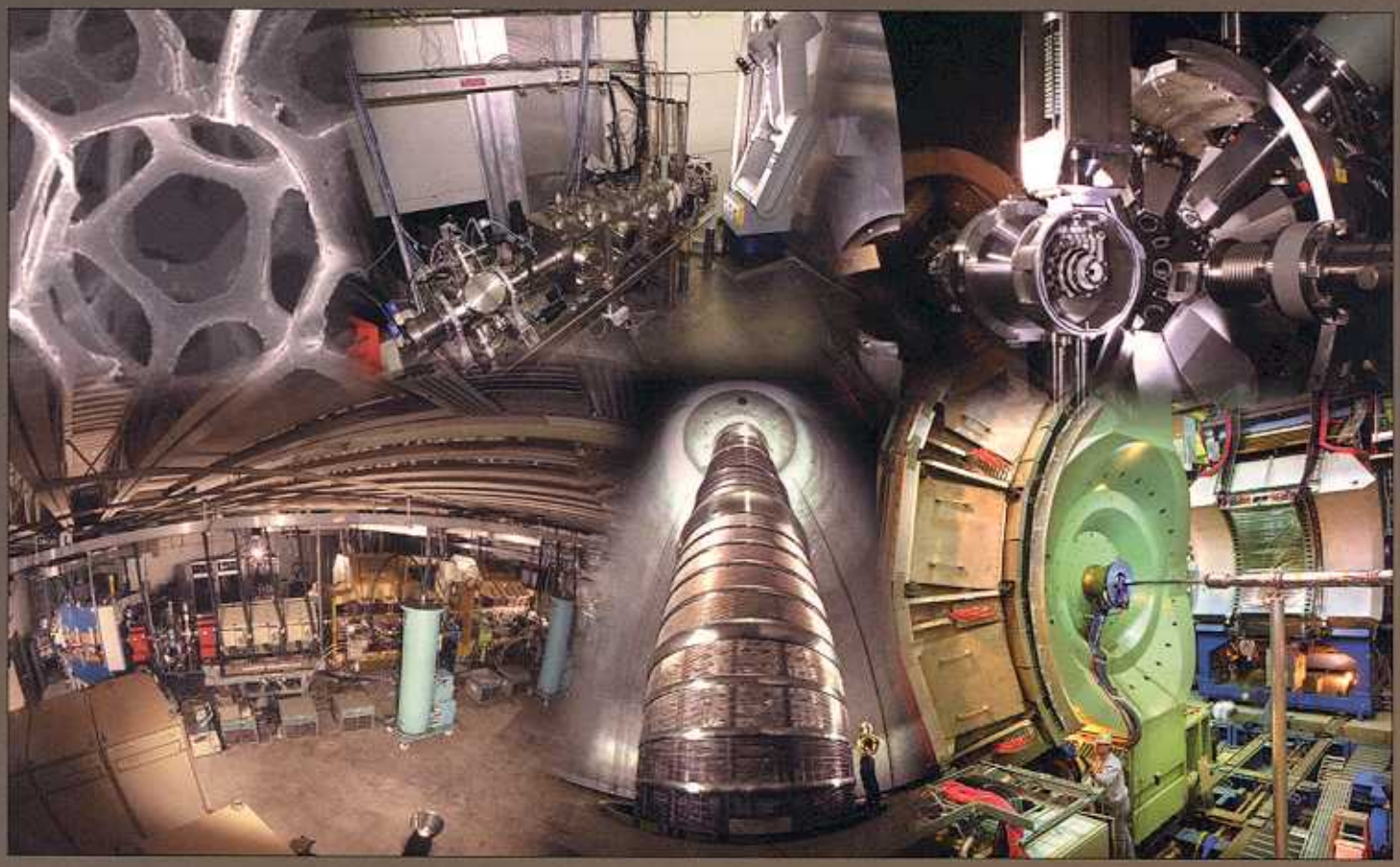

A publication of NuPECC, an Associated Committee of the European Science Foundation, with colleagues from EPS-NPB, Europe, America and Asia

The Nuclear Liquid-Gas Phase Transition: Studies with the ISiS Array

The study of multifragmentation and its possible link to a nuclear liquid-gas phase transition has been motivated by the desire to understand the nuclear equation of state, with its broad applications to nuclear physics and astrophysics. Nuclear fragmentation reactions first became of interest in the 1950s as a result of radiochemical and emulsion measurements conducted with hadron beams [1–3]. However, detector technology and data-acquisition capabilities permitted only inclusive investigations of these complex reactions until the late 1970s. In a set of key experiments at Fermilab and the Brookhaven AGS, the Purdue group measured complete spectra and isotope yields from bombardments of heavy nuclei with 1–300 GeV protons [4]. While these experiments lacked the multiparticle detection capability needed to confirm the existence of a phase transition, they stimulated extensive scientific discourse about this possibility. Further, the results spurred construction of several large 4π detector arrays dedicated to the search for the nuclear liquid-gas phase transition in both hadron- and heavy-ion-induced reactions [5].

The Indiana Silicon Sphere (ISiS) project was initiated in the late 1980s in order to focus on light-ion induced reactions. Light ions, especially hadrons, are particularly advantageous for multifragmentation studies since they emphasize the thermal properties of the disintegrating residue, with minimal rotational and compressional effects. Experimentally, one also has the advantage of producing a broad, continuous distribution of excitation energies in a single reaction and observing the breakup in a reference frame very close to the center-of-mass system. To search for evidence of a phase transition, a 4π detector was required in order to provide fragment multiplicity information, event topology and calorimetry.

Because the previous studies [4, 6] had shown a broadening to low energies in the kinetic energy spectra of the clusters (IMFs: $3 \leq Z \leq 20$) emitted in reactions above several GeV bombarding energy), the detector design also demanded very low thresholds and good energy resolution. Thus, it was decided to construct a silicon-based array augmented by low pressure gas-ionization chambers for Z-identification of the lowest energy fragments and a CsI scintillator with photodiode readout for Z and A identification of the energetic lighter fragments, shown in Figure 1 and described in [7]. Consistent with light-ion kinematics, a spherical geometry was chosen for the 162 close-packed triple telescopes in the array, arranged in nine concentric rings, each containing 18 detector modules. A schematic of the ISiS array is shown in Figure 2. The detector configuration yielded a kinetic energy acceptance of 1 MeV $\leq$ E/A $\leq$ 92 MeV for charge-identified fragments up to Z = 16; Z and A identification for 8 MeV $\leq$ E/A $\leq$ 92 MeV products, and "grey particle" detection for fast particles (primarily protons and pions) up to 350 MeV. Some development of the detector modules proceeded in parallel with our Saclay colleagues, who were also involved in the development of the silicon modules for the INDRA array for heavy-ion measurements.

Four campaigns were carried out with the ISiS array: E228 at LNS Saclay with 1.8–4.8 GeV ^{3}He ions; E375 at IUCF with 130–260 MeV proton and ^{3}He beams; E900 at AGS with 5.0–14.6 GeV/c proton and π^- beams, and E900a at AGS with 8.0 GeV/c tagged antiproton and π^- beams. Principal experimentalists involved in the collaboration included former members of the IU group (L. Beaulieu, D. S. Bracken, E. Foxford, T. Lefort, and K. B. Morley) and scientists from Simon Fraser University

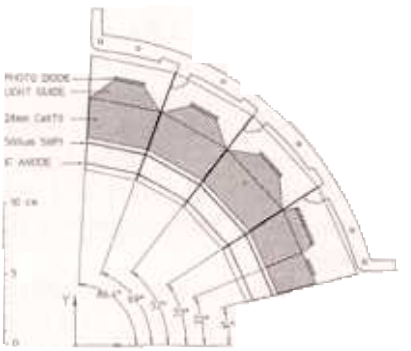

Figure 1. *Drawing of an ISiS arc bar for the forward hemisphere, with the angular coverage of each telescope labeled. Each unit is a part of an 18-member ring; the forward-most element is divided into two segments. Rings are identified as follows: 14–22° (1A); 22–33° (1B); 33–52° (2); 52–69° (3); 69–86.4° (4); 93.6–111° (5); 111–128° (6); 128–147° (7); 147–166° (8).*

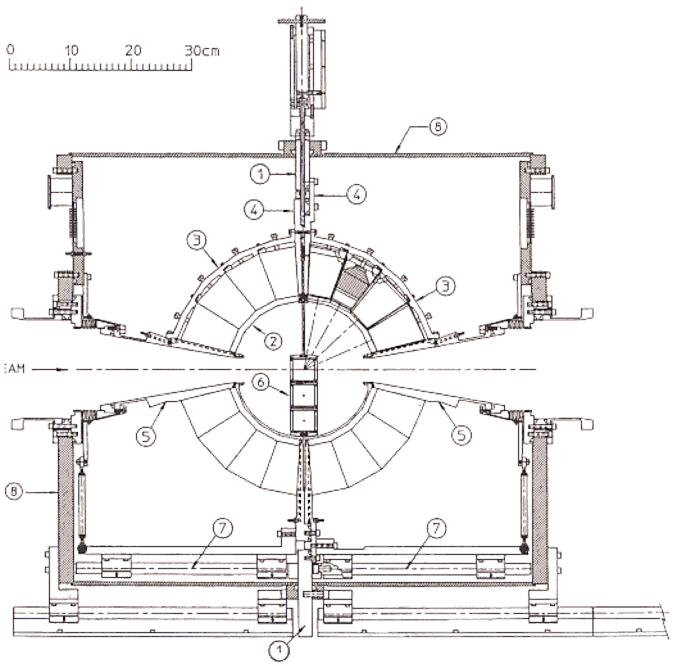

Figure 2. *Assembly drawing of the ISiS system. Components are as follows: (1) center ring, (2) window, (3) arc bars, (4) center disks, (5) support cones, (6) target ladder assembly, (7) steel rails, and (8) vacuum chamber.*

(R. G. Korteling), CEA Saclay (C. Volant, R. Legrain, and E. C. Pollacco), Texas A&M University (S. J. Yennello and A. Ruangma), Jagiellonian University (J. Brzychczyk), the University of Maryland (H. Breuer), and Warsaw University (L. Pienkowski).

The clearest signatures of a phase transition are found in the AGS data, in particular the 8.0 GeV/c π^- + ^{197}Au reaction, where 2.5×10^6 events with multiplicity $M \geq 3$ for thermal-like charged particles were recorded. These data exhibit several experimental criteria characteristic of a thermalized system undergoing a phase transition. First, the fragments are emitted nearly isotropically and exhibit Maxwellian-like kinetic energy spectra. This behavior is illustrated in the differential cross section plots for carbon fragments in Figure 3 as a function of the heat content, excitation energy per residue nucleon E*/A, of the hot target residue [8]. One observes that as E*/A increases, the spectra are broadened toward lower and lower energies, consistent with the breakup of a system with lower than normal nuclear density.

The fragment multiplicities and size distributions are also important criteria. Figure 4 shows the evolution of the emitting source charge and the charges of the three largest fragments as E*/A increases. For $E^*/A \lesssim 4$–5 MeV, which comprises ~95% of the total reaction cross section, Figure 4 indicates that the events are associated with a heavy residue, consistent with evaporative emission. At higher excitation energies the tendency is for each event to produce fragments of increasingly similar sizes, so that above $E^*/A \gtrsim 6$ MeV, multifragmentation into

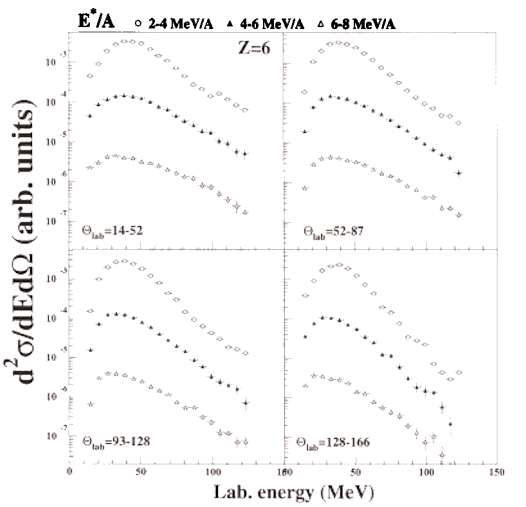

Figure 3. *Kinetic-energy spectra of oxygen nuclei at four angles in the laboratory system for three bins of excitation energy for 8 GeV/c π^- + ^{197}Au reaction; open circles are for E*/A = 2–4 MeV; closed triangles for E/A = 4.6 MeV; open triangles for E*/A = 6–9 MeV. The lines correspond to SMM calculations for breakup volume $V = 3V_0$ with extra expansion energy, equal to zero (solid line) and 0.5A MeV (dashed line) [10]. For each bin in excitation energy the simulated spectrum is normalized to the maximum of the experimental one.*

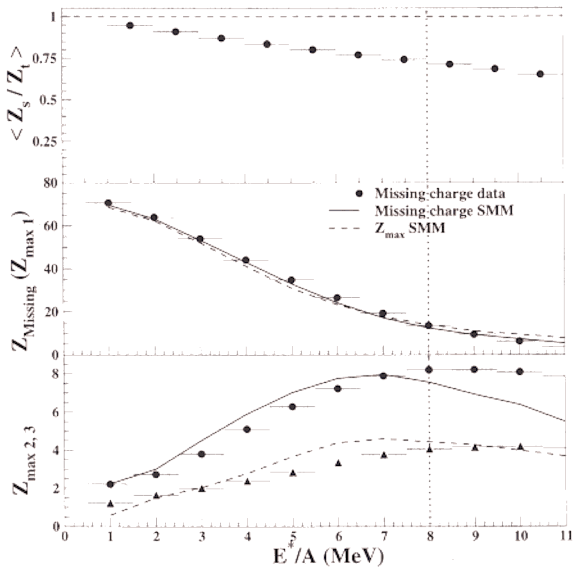

Figure 4. *Dependence of fractional source charge and IMF charges as a function of E*/A for the 8 GeV/c π^- + ^{197}Au reaction [16]. Top: Fractional source charge of residue. Middle: Missing charge in ISiS, assumed be the largest fragment; and SSM prediction for missing charge (solid line) and for largest fragment (dashed line), both passed through the ISiS filter. Bottom: Charge of two largest observed fragments; solid line is the SMM prediction for second largest fragment ($Z_{max}2$), and dashed line, for third largest fragment ($Z_{max}3$).*

IMFs and light-charged particles is the dominant process. The upper panel of Figure 5 shows how the probability for a given IMF multiplicity depends on E*/A (the undetected largest residue is not included). In the second frame the corresponding charge distributions have been fit with a power law; $\sigma(Z)\alpha Z^{-\tau}$. A minimum in the power-law exponent τ is observed near E*/A ~ 6 MeV, indicating a tendency to form increasingly large clusters up to this point. This minimum signals the possible onset of a phase transition, as discussed in [9] and [10]. At higher excitation energies, the cluster sizes begin to decrease, in part due to secondary decay of the hot fragments.

The breakup time scale is central to distinguishing between the "instantaneous" breakup associated with a phase transition and a slower sequential evaporative process. In the bottom frame of Figure 5, the evolution of the relative emission time for IMFs is shown as a function of E*/A [11]. At low excitation energy, the time scales are relatively long, typical of evaporative emission. However, with increasing E*/A the time scale decreases rapidly, reaching values of $\Delta\tau$ ~ 20–50 fm/c for E*/A $\gtrsim$ 4 MeV; i.e., the breakup is nearly instantaneous. In this same excitation energy range, the third panel shows evidence for a slight extra thermal expansion energy [12], much smaller than the compression-induced values found in collisions between mass-symmetric heavy-ion studies. All of the above observables—multiplicity and charge distributions, time scale, and extra thermal expansion energy—indicate a mechanism change near E*/A ~ 4–6 MeV, corresponding to the predicted threshold from multifragmentation models [13–15].

When temperatures derived from double isotope ratios are plotted versus the heat content of the system (the caloric curve), the ISiS data exhibit behavior similar to the heating of a liquid to the boiling point, as originally shown by Pochodzalla et al. [16] for the ALADIN results. Further analysis suggests evidence for a negative heat capacity at the liquid-gas transition point, consistent with the recent results of D'Agostino et al. [17]. In both cases a first-order phase transition is consistent. Beaulieu et al. [18] showed that the ISiS data exhibit binomial reducibility and thermal scal-

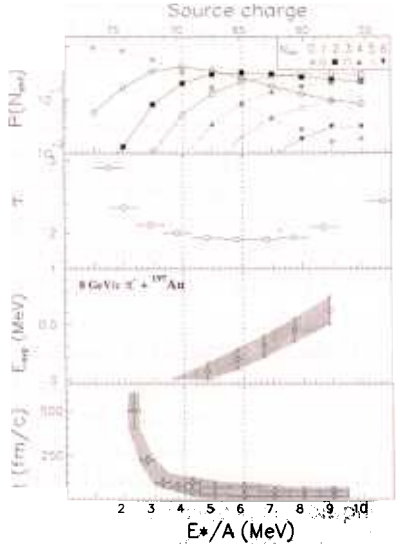

Figure 5. *Dependence on E*/A for the following qualities, from bottom up: relative IMF emission time t, extra radial expansion energy E_{exp}/A_{IMF}, charge distribution power law exponent τ and probability for a given IMF multiplicity [16].*

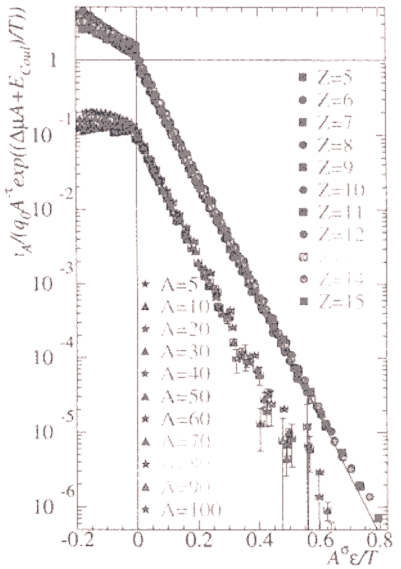

Figure 6. *The scaled yield distribution versus the scaled temperature for the ISiS data (upper) and d = 3 Ising model calculation (lower) from [10]. For the Ising model the quantity* $(n_A/q_0A^{-\tau})/10$ *is plotted against the quantity* $A^{\sigma}\varepsilon/1.435T$. *Data for* $T > T_c$ *is scaled only as* $n_A/q_0A^{-\tau}$.

ing, adding support for the case of statistical concepts in evaluating the data. General agreement with nuclear multifragmentation models has also been obtained using the calculations of Botvina et al. [13] and Friedman [14].

However, perhaps the most compelling evidence for a nuclear liquid-gas phase transition may lie in the ability to describe the distributions with more general statistical theories of liquid-gas properties. Using a percolation model, Berkenbusch et al. [9] have shown evidence for a continuous phase transition, with the expected critical parameters, for the mass distribution of 10.2 GeV/c protons incident on ^{197}Au. At the same time, Elliott et al. [10] applied a

References

1. N. A. Perfilov, O. V. Lozhkin, and V. P. Shamov, *Sov. Phys. Usp.* **3**, 1 (1960).
2. J. Hudis, in *Nuclear Chemistry,* edited by L. Yaffe (Academic Press, New York, 1968).
3. W. G. Lynch, *Ann Rev. Nucl. Part. Sci.* **37**, 493 (1987).
4. N. T. Porile et al., *Phys. Rev. C* **39**, 1914 (1989).
5. See, for example, Nucl. Phys. A681, 267c (2001) and *Proc. of Int. Workshop XXVII on Gross Properties of Nuclei and Nuclear Excitations: Multifragmentation,* Jan. 1999 (GSI Darmstadt, DE, edited by H. Feldmeier, J. Knoll, W. Norenberg and J. Wambach).
6. S. J. Yennello et al., *Phys. Rev. Lett.* **67**, 671 (1991).
7. K. Kwiatkowski et al., *Nucl. Instr. Meth. A* **360**, 571 (1995); A. Ruangma et al. submitted to Phys. Rev. C.
8. T. Lefort et al., *Phys. Rev. C* **64**, 064603 (2001); L. Beaulieu et al., Phys. Rev. C 64, 064604 (2001).
9. M. Berkenbusch et al., *Phys. Rev. Lett.* **88**, 022701 (2002).
10. J.B. Elliott et al., *Phys. Rev. Lett.* **88**, 042701 (2002).
11. L. Beaulieu et al., *Phys. Rev. Lett.* **84**, 5971 (2000).
12. T. Lefort et al., *Phys. Rev. C* **62**, 0316(R) (2000).
13. A. Botvina, A. S. Iljinov and I. N. Mishustin, *Nucl. Phys. A* **507**, 649 (1990).
14. W. Friedman, *Phys. Rev. C* **42**, 667 (1990).
15. D. H. E. Gross, *Rep. Prog. Phys.* **53**, 605 (1990).
16. J. Pochodzalla et al., *Phys. Rev. Lett.* **75**, 1040 (1995).
17. M. D'Agostino et al., *Phys. Lett. B* **473**, 219 (2000).
18. L. Beaulieu et al., *Phys. Rev. C* **63**, 031302 (2001).

V. E. Viola
IUCF and Department of Chemistry
Indiana University
Bloomington, IN, USA

K. Kwiatkowski
Physics Division
Los Alamos National Laboratory
Los Alamos, NM, USA